ORIGINAL ARTICLE

A pilot-scale rotary infrared dryer of shrimp (*Metapenaeus affinis*): Mathematical modeling and effect on physicochemical attributes

Asaad R. Al-Hilphy[1] ⓘ | Atheer Abdul Amir Al-Mtury[2] | Sajedah A. Al-Iessa[1] | Mohsen Gavahian[3] ⓘ | Sabah Malik Al-Shatty[1] | Muhammad Ali Jassim[1] | Zainab Abdul Ameer Mohusen[1] | Amin Mousavi Khaneghah[4] ⓘ

[1]Department of Food Science, College of Agriculture, University of Basrah, Basrah, Iraq

[2]Basrah Agricultural Directorate, Basrah, Iraq

[3]Department of Food Science, National Pingtung University of Science and Technology, Pingtung, Taiwan, Republic of China

[4]Department of Food Science and Nutrition, Faculty of Food Engineering, State University of Campinas (U.N.I.C.A.M.P.), Campinas, São Paulo, Brazil

Correspondence
Mohsen Gavahian, Department of Food Science, National Pingtung University of Science and Technology, 1, Shuefu Road, Neipu, Pingtung 91201, Taiwan, Republic of China.
Email: mohsengavahian@yahoo.com

Amin Mousavi Khaneghah, Department of Food Science and Nutrition, Faculty of Food Engineering, State University of Campinas (U.N.I.C.A.M.P.), Campinas, São Paulo, Brazil.
Email: mousavi@unicamp.br; mousavi.amin@gmail.com

Abstract

A new rotary infrared dryer (R.I.D.) was manufactured to dry shrimp (*Metapenaeus affinis*) at 60, 70, and 80°C. Also, mathematical modeling along with artificial neural networks (ANNs) was used for data prediction. The results showed that the exponential proposed model and ANN could be applied to well-predict the moisture ratio of shrimp. Besides, running R.I.D. at 80°C resulted in the highest reduction in moisture content and saved about 42% of drying time. The thermal efficiency of the R.I.D. at a temperature of 70°C ranged between 83 and 89%, which was about 15% higher than the conventional dryer. The drying rate by both R.I.D. and conventional methods consist of a falling rate period, ranging between 1.68×10^{-4} and 0.47×10^{-4} 1/s. Furthermore, the mass transfer coefficient increased by about 104.6% when drying temperature increased from 60 to 80°C. The browning index increased with the increase of drying temperature. Specific energy consumption, browning index, and drying time of rotary infrared system were lower than those of conventional system by 46.9, 33.3, and 34.7%, respectively. R.I.D. reduced energy consumption, decreased the color changes, improved the rehydration ratio, and affected the chemical composition of dried shrimp as compared with the conventional process.

Practical Applications

A new rotary infrared dryer was designed and developed and its performance was evaluated with the assistance of artificial neural networks. This system was shown to be energy- and time-saving and capable of producing high-quality dry shrimp (*Metapenaeus affinis*). Also, the system is simple and affordable due to reducing energy consumption and relatively low cost of components. Therefore, it has the potential to be used in the industry after further economic and technical evaluation.

1 | INTRODUCTION

Shrimp is a rich source of calcium, vitamins, protein, extractable compounds, vitamin B12, selenium, omega-3, highly unsaturated fatty acids, and astaxanthin. Also, it has a natural flavor and is considered a segment in the salad, pasta curry, soup, stir-fried dishes, but it has low calories and saturated fat (Gökoğlu, 2021). Drying is an effective and cheap method of food preservation, in addition to the convenience of preservation, and the flavor of dried shrimp is desirable (Guochen, Arason, & Arnason, 2010) and reduces enzymes activity due to

reducing water activity (Gökoğlu, 2021). Besides, artificial network (ANN) is a promising approach that effectively alleviates the model mismatch problem to produce a suitable topology as a predictive time-saving, and efficient methodology (Li & Chen, 2019).

The purpose of drying shrimp is to reduce the moisture content to a minimum level and inhibit enzymes and other biological reactions. Also, whole or powder-dried shrimp are used in soups and sauces as the primary protein source because of their delicious flavor (Akonor, Ofori, Dziedzoave, & Kortei, 2016). Several methods have been used to dry shrimp, such as heat pump drying (Shamsuddeen, Cha, Kim, & Kim, 2020), freeze-drying (Dons et al., 2001), and hot air convection drying (Ersan & Tugrul, 2020). These drying methods need high energy and operation cost (Aniesrani Delfiya, Murali, Alfiya, & Samuel, 2020; Murali et al., 2021). In this regard, solar drying is eco-friendly, but it needs a long time. At the same time, natural sun drying causes pollution for shrimp such as dust, rains, microorganisms, and attacked by insects. Therefore, bed infrared radiation shrimp drying (Delfiya et al., 2021) is used, but it needs to flip the shrimp manually during drying to enhance heat and mass transfer. This operation needs extra time to complete the drying process. Silva, Nogueira, Duarte, and Barrozo (2021) utilized a roto-aerated dryer for drying acerola and used infrared as a pre-drying system. Infrared drying is one of the most promising methods and environmentally friendly (Aboud, Altemimi, Al-Hilphy, Yi-Chen, & Cacciola, 2019).

Although several reports in the literature on drying shrimp, there is no report on drying shrimp with an infrared rotary dryer. The present study aims to design a rotary infrared dryer (R.I.D.) and study its effect on dried shrimp's chemical and physical characteristics. In addition, the proposed exponential model and ANN model were applied to predict moisture ratio.

2 | MATERIALS AND METHODS

2.1 | Sample preparation

Fresh white shrimp (*Metapenaeus affinis*) with 200–207 shrimp/kg, and dimensions of shrimp are the length of 10 ± 0.23 cm, and diameter of 4.4 ± 0.16 cm. shrimp was purchased from a local seafood market (Basrah, Iraq). About 4.5 kg of fresh shrimp was used in the present study, divided into four groups. Each group was replicated three times. The shrimp were thawed at 4°C for 24 hr then deshelled and washed. The shrimp was immersed in salt solution (2% wt/vol) for 2 min for reducing microorganisms (Hosseinpour et al., 2013). After that, the samples were cooled by ambient air for 5 min and used in the drying experiments. For moisture content of shrimp determination, 60.94 g of raw shrimp was dried in an oven (Binder, ED23, GmbH, Germany) with an accuracy of 0.5°C at 105°C till it reached the constant weight (AOAC International, 2016). Average moisture content reached 81.1%.

2.2 | Rotary infrared dryer

R.I.D. (Figures 1 and 2) was designed and fabricated in the Food Engineering Laboratory, University of Basrah, Iraq. It consists of an infrared lamp (250 W, 6 μm wavelength, model PAR38, China), a rotary operated cylinder with a length of 37 cm, and a diameter of 15 cm fixed into the dryer. The cylinder is connected with an electric motor (Leison motor, Model No. KXTYZ-1, China) with 6 W power and its speed of 2 rpm. The dryer contains a fan (50 W, 2,500 rpm, model J238-11154, China) to move air and enhance forced convection heat transfer. The dryer was provided with a digital temperature gauge to control the drying temperature (range temperature of the thermostat (0–300°C) (labor, lab_3456760, India). The capacity of the cylinder is 1 kg of raw food. The dryer body was made of wood covered with aluminum foil to reflect infrared radiation on the cylinder—Table 1 summarized the R.I.D. design dimensions.

2.3 | Conventional dryer

A natural convection binder drying oven (Binder, ED23, GmbH) was used for drying shrimp samples at 80°C temperature. The oven provided with a digital temperature controller (temperature range: +5°C above ambient temperature to +300°C), fan, port to output moist air, 2 chrome-plated racks, and electric heater (230 V 1–50/60 Hz). The experiments were replicated three times.

2.4 | Drying process of shrimp

The initial weight of samples in each treatment was 375 g of fresh shrimp. These batches were dried by the conventional oven and R.I.D. The change of shrimp weight with drying time (the interval time was 10 min) was recorded using a digital balance scale (CGOLDENWALL, LST-JM-103), with an accuracy of 0.01 g the change of moisture content during drying time was determined.
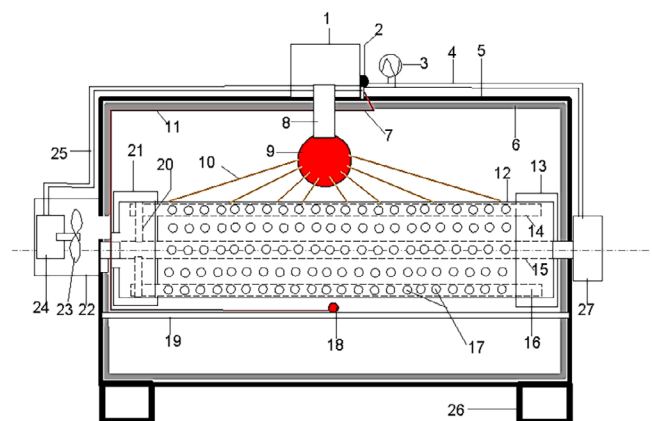

FIGURE 1 The layout of the rotary infrared dryer. 1. Cover, 2. thermostat, 3. electrical current source, 4 and 25. electrical wires, outside body of dryer, 6. aluminum foil, 7 and 11. capillary pipe of thermostat, 8. lamp base, 9. infrared lamp, 10. infrared radiation, 12. rotary cylinder, 13 and 21. cylinder cover, 14 and 16. partitions, 15. rotor shaft, 17. cylinder ports, 18. the sensor of the thermostat, 19. supporting plate, 20. bearing of rotor shaft, 22. cover, 23. fan, 24. electrical motor, 26. base, 27. electrical motor of the cylinder
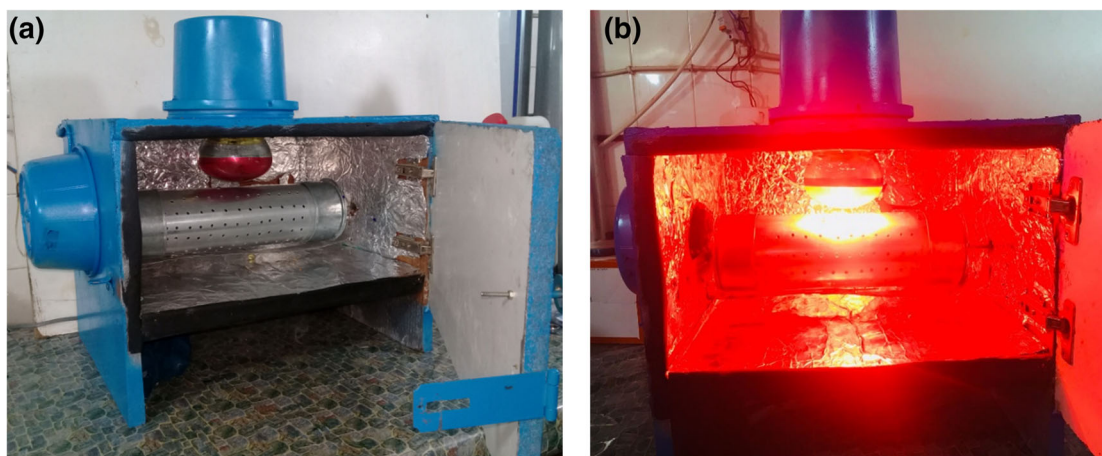
FIGURE 2 Photograph of the rotary infrared dryer (a) before operation and (b) during operation

TABLE 1 Design specifications of the rotary infrared dryer

Component/specification	Value/unit
Infrared lamp	250 W
Length of rotary operated cylinder	37 cm
Diameter of rotary operated cylinder	15 cm
Capacity of rotary operated cylinder	1 kg of raw food per batch
Electric motor	6 W
Rotation speed of electric motor	2 rpm
Fan	50 W
Rotation speed of fan	2,500 rpm
Thermostat	0–300°C
Body of dryer	Wood covered by aluminum foil

2.5 | Drying rate

Drying rate is the rate of the quantity of removed moisture from shrimp with time during drying. The drying rate was calculated according to Equation (1). As below (Doymaz, 2011):

$$DR = \frac{M_{t+dt} - M_t}{dt} \tag{1}$$

where DR is the drying rate (g_{water}/min), M_{t+dt} is the moisture content (g_{water}/g dm) at $t + dt$ after the time (t), M_t is the moisture content (g_{water}/g dm) at t time (min).

2.6 | Thermal efficiency

Thermal efficiency is the ratio of required heat energy to evaporate water from shrimp to the provided energy to the dryer. Thermal efficiency is given in Equation (2) (Earle, 1983):

$$\eta = \frac{T_d - T_o}{T_d - T_a} \times 100 \tag{2}$$

where η is the thermal efficiency (%), T_d is the drying temperature (°C), T_o is the outlet air temperature from the dryer, and T_a is the ambient temperature (°C).

2.7 | Specific energy consumption

Specific energy consumption (S.E.C.) is the required energy to eliminate 1 kg of water from raw shrimp. S.E.C. was calculated from the following equation (Raso et al., 2016).

$$SEC = \frac{VIt}{m} \tag{3}$$

where S.E.C. is the specific energy consumption (kJ/kg), V is the voltage (V), I is the current (A), t is the time (s), m is the evaporated water from shrimp during drying (kg). To convert unit of S.E.C. to kJ/kg, it was divided on 1,000.

2.8 | Color measurement

Color is a very important parameter that a consumer uses to assess food products' overall appearance and quality. Color is also highly regarded by the processing industry due to its effect on food selects. The image processing method was used to analyze the color characteristics of the dried shrimp. Images of fresh and dried shrimp were taken with a high-resolution digital camera (8 megapixels) (IP67 Endoscope, Mileseey, China) under appropriate lighting as described in the literature (Al-Hilphy et al., 2021). ImageJ software was used to obtain the picture color values (L, a, and b) and then corrected to L*, a*, and b* according to Yam and Papadakis (2004).

The color change of dried shrimp was calculated from the following equation (Gavahian, Chu, & Farahnaky, 2019):

$$\Delta E = \sqrt{(L_o{}^* - L^*)^2 + (a_o{}^* - a^*)^2 + (b_o{}^* - b^*)^2} \quad (4)$$

where ΔE is the color change, L^* is the lightness, a^* is the redness/blueness, and b^* is the yellowness/greenness, respectively, for fresh shrimp. While L^*, a^*, and b^* are used for dried shrimp.

Chroma (ΔC) was calculated from Equation (5) (Wrolstatad & Smith, 2017):

$$\Delta C = \sqrt{(a_o{}^* - a^*)^2 + (b_o{}^* - b^*)^2} \quad (5)$$

Hue angle was calculated according to Equation (6) (Wrolstatad & Smith, 2017):

$$h = \tan^{-1}\frac{b^*}{a^*} \quad (6)$$

where h is the hue angle (°) and L^*, a^*, and b^* are the lightness, redness/blueness, and yellowness/greenness, respectively.

2.9 | Browning index

Browning index (BI), defined as brown purity, is one of the most common indicators of browning in sugar-containing food products. BI was calculated by Equation (7) as follows (Mikulec, Kowalski, Makarewicz, Skoczylas, & Tabaszewska, 2020):

$$BI = \frac{[100(X - 0.31)]}{0.172} \quad (7)$$

$$X = \frac{(a^* + 1.75L^*)}{(5.645L^* + a^* - 3.012b^*)} \quad (8)$$

where L^*, a^*, and b^* are the lightness, redness/blueness, and yellowness/greenness, respectively.

2.10 | Rehydration ratio

The rehydration ratio is the ratio of the mass of the rehydrated, drained-out shrimp to the mass of the original shrimp. According to Doymaz and İsmail's (2011) method, the dried shrimp meat was rehydrated with some modifications. Then, 5 g of dried shrimp meat was rehydrated in distilled water at room temperature using a sample of water (1:40). At 5-min interval, the shrimp meat was removed, carefully dried with paper towels, weighed with an electronic scale (different 5 g samples for every 5 min interval were used). Dried shrimps were rehydrated over 85 min when the weight of the rehydrated

samples stabilized. Then, the rehydration ratio was calculated using Equation (9) as follows (Lewicki, 1998):

$$R_r = \frac{w_r}{w_{ad}} \quad (9)$$

where R_r is the rehydration ratio, w_r is the mass of dried shrimp after rehydration (g), and w_{ad} is the mass of dried shrimp after drying.

2.11 | Mathematical modeling

Many considerations must be taken while using mass transfer equations and mathematical modeling in food dryings, such as negligible shrinkage and deformation during drying, the drying process isotherm, and diffusion is used for mass transfer mechanism (Simal, Deya, Frau, & Rossello, 1997). In the current study, thin-layer drying models were associated with moisture ratio (dimensionless) on dry matter. Mathematical models are used for exploring the relationship between drying time and moisture ratio. Table 2 depicts the fits of 16 thin-layer drying mathematical models on the moisture ratio versus drying time. The constants of mathematical models are k, c, n, a, k_o, k_1, b, k_2, g, k_3, and L, as shown in Table 2. RMSE and R^2 were used to evaluate the fitting model on the experimental data. The best fitting of the model has a lower RMSE and higher R^2. RMSE and R^2 were given in Equations (10) and (11) as follows:

$$R^2 = \frac{\sum\limits_{i=1}^{N}\left(MR_{pre.} - \overline{MR_{pre.}}\right)^2}{\sum\limits_{i=1}^{n}\left(MR_{exp.} - \overline{MR_{exp.}}\right)^2} \quad (10)$$

$$RMSE = \left[\frac{\sum\limits_{i=1}^{N}\left(MR_{exp.} - MR_{pre.}\right)^2}{N}\right]^{1/2} \quad (11)$$

where R^2 is the correlation coefficient, $MR_{pre.}$ is the predicted moisture ratio, $MR_{exp.}$ is the expected moisture ratio, $\overline{MR_{pre.}}$ is the mean of predicted moisture ratio, $\overline{MR_{exp.}}$ is the mean of expected moisture ratio, RMSE is the root mean square error, and N is the number of observations.

2.12 | ANN modeling

A multiple layer forward back propagation neural network model was utilized to predict moisture ratio. The input variable was drying time (one neuron input layer), and the output variable was moisture ratio (neuron output layer), as illustrated in Figure 3. A 75 and 25% of data were used for training and testing, respectively, randomly selected. S.P.S.S. ver. 21 was applied in the present study. ANN was trained (Training aims to reduce the error function by looking for a set of

TABLE 2 Mathematical models were applied in the drying curves of shrimp

Model name	Model	Reference
Lewis model	$MR = \exp(-kt)$	Demir, Gunhan, and Yagcioglu (2007)
Al-Hilphy et al.	$MR = (a + kt)^{-1/c}$	Al-Hilphy et al. (2021)
Page model	$MR = \exp(-kt^n)$	Page (1949)
Modified page model	$MR = \exp\left[-(kt)^n\right]$	Menges and Ertekin (2006)
Henderson and Pabis	$MR = a\exp(-kt)$	Hendorson and Pabis (1961)
Logarithmic model	$MR = \exp(-kt) + c$	Yagcioglu et al. (1999)
Two-term model	$MR = \exp(-k_o t) + b\exp(-k_1 t)$	Madamba, Driscoll, and Buckle (1996)
Approximation of diffusion	$MR = \exp(-kt) + (1 - a)\exp(-kbt)$	Yaldýz and Ertekýn (2001)
Wang and Singh	$MR = 1 + at + bt^2$	Wang and Singh (1978)
Midilli	$MR = a\exp(-k(t^n)) + bt$	Midilli, Kucuk, and Yapar (2002)
Two-term exponential	$MR = \exp(-kt) + (1 - a) + \exp(-kat)$	Sharaf–Eldeen et al. (1980)
Verma et al.	$MR = a\exp(-kt) + (1 - a)\exp(-gt)$	Verma, Bucklin, Endan, and Wratten (1985)
Modified Henderson and Pabis	$MR = a\exp(-k_1 t) + b\exp(-k_2 t) + c\exp(-k_3 t)$	Karathanos (1999)
Simplified Fick's diffusion	$MR = \exp\left(-c\left(t/L^2\right)\right)$	Diamante and Munro (1993)
ANN	—	Proposed
Exponential	$MR = e^{\left(a + \frac{b}{t + c}\right)}$	Proposed

Abbreviation: AAN, artificial neural network.

connections weights and biases that make the ANN output equal or close to the target data.) with the hyperbolic tangent function. The hyperbolic tangent function was used as a transfer function in each hidden layer (Hernandez-Perez, Garcıa-Alvarado, Trystram, & Heyd, 2004), and the linear transfer function has been used in the output layer. To minimize error, Levenberg–Marquardt algorithm was used. Several hidden layers and neurons were varied from 5 to 6. The network in the present study stopped at a minimum of the sum of square error. The determination coefficient (R^2) and mean square error (MSE) utilized to minimize the error function (Momenzadeh, Zomorodian, & Mowla, 2011):

$$MSE = \frac{\sum_{P=1}^{M}\sum_{i=1}^{N}(S_{IP} - T_{IP})^2}{MN} \quad (12)$$

where N is the number of output layer neurons, S_{IP} is the output ANN of neuron i and pattern p, T_{IP} is the output of goal in neuron i and pattern p, and M is the number of test patterns.

2.13 | Mass transfer coefficient

Fick's second law-governed moisture diffusion process during drying. Many assumptions for this process are finite as internal and external resistance to moisture transfer through the sols, drying medium, and thermophysical characteristics of the solid are constant. The moisture loss is not affected by heat transfer, the moisture diffusion in one direction, and the transient moisture diffusivity model in Cartesian coordinates with dimensionless. According to Dincer and Hussain (2002), the moisture ratio is given in Equation (13):

$$MR = \sum_{n=1}^{\infty} A_n B_n \quad (13)$$

Equation (13) can be simplified to Equation (14) (a first term only) when the values of $\mu_1^2 Fo > 1.2$ are small and negligibly.

$$MR = A_n B_n \quad (14)$$

where MR is the moisture ratio, ($A_n = A_1$ and $B_n = B_1$):

Because the shape of shrimp is cylindrical, the following equation can be used:

$$A_1 = \exp.\left[\frac{0.5066 Bi}{17 + Bi}\right] \quad (15)$$

where Bi is the Biot number.

Equation (16) can be used for all objects as follows:

$$B_1 = \exp.\left(-\mu_1^2 Fo\right) \quad (16)$$

where Fo is the Fourier number.

Moisture ratio can be calculated from Equation (17) (Dincer & Dost, 1996):
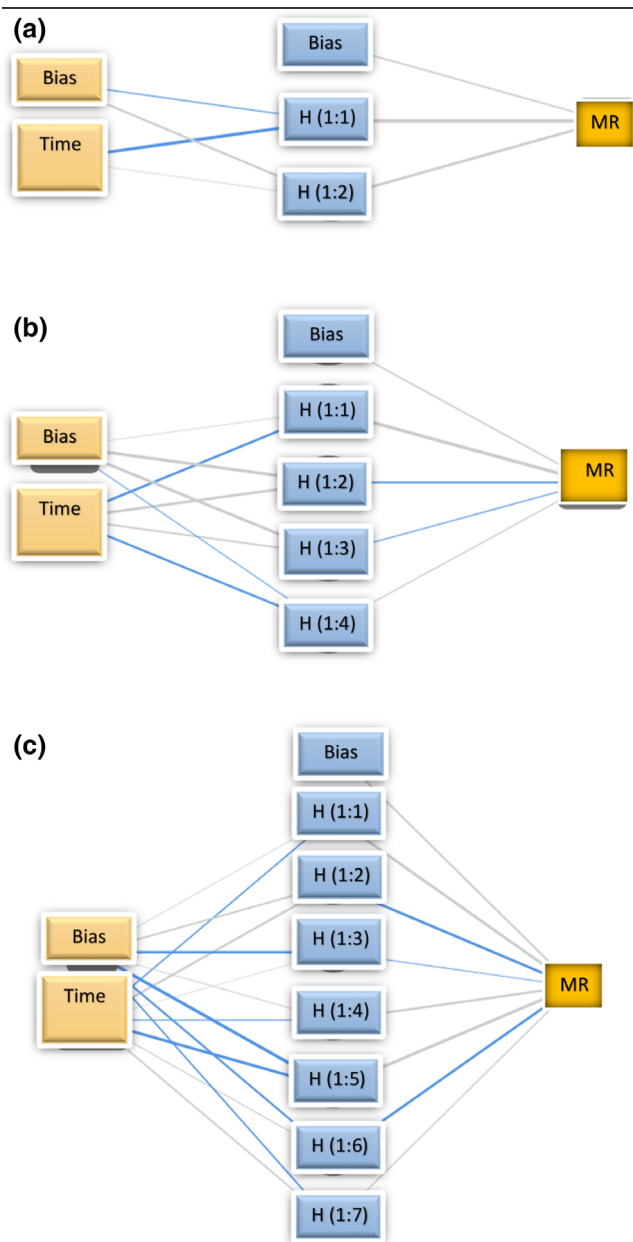
$$MR = A\exp(-kt) \quad (17)$$

FIGURE 3 Artificial neural network (ANN) structure for predicting moisture ratio (MR) of dried shrimp. (a) 60, (b) 70, and (c) 80°C temperatures

where A is the lag factor, k is the drying coefficient (1/s), and t is the time (s).

Moisture ratio can be obtained from experimental moisture content data according to Equation (18):

$$MR = \frac{M - M_e}{M_i - M_e} \quad (18)$$

where M is the moisture content at a specific time (g water/g dm), M_e is the equilibrium moisture content (g water/g dm), and M_i is the initial moisture content (g water/g dm).

Moisture diffusivity is given by Equation (19) (Dincer & Dost, 1996):

$$D = \frac{k L^2}{\mu_1^2} \quad (19)$$

where D is the moisture diffusivity (m²/s) and L is the radius of cylindrical (m).

μ is the root of solution to the moisture diffusivity, and it is calculated from Equation (20) (Dincer & Hussain, 2002):

$$\mu_1 = \left[\left(\frac{3}{4.188}\right)\ln(6.796Bi + 1)\right]^{1/1.4} \quad (20)$$

Biot number and Fourier number are defined as:

$$Bi = \frac{h_m L}{D} \quad (21)$$

$$Fo = \frac{Dt}{L^2} \quad (22)$$

Bi, Fo, and h_m are the Biot number, Fourier number, and mass transfer coefficient, respectively.

2.14 | Chemical composition

The chemical composition of shrimp included moisture content, protein, fat, ash, and carbohydrate. It is very important, as it is possible, to know the effect of the drying method on it. Chemical composition was determined according to AOAC International (2016) as follows: Moisture content was determined by using an oven (Binder, ED23, GmbH) at 105°C for 3 hr for the shrimp samples. The percentage of fat was estimated by the Soxhlet (Gerhardt, EV6 AIL/16, Germany). Ash was estimated by burning samples in a Muffle Furnace (Carbolite-S30.2AU, England) at 550°C for 16 hr. For protein determination, the percentage of total nitrogen was estimated according to the Semi-Micro Kjeldahl Nitrogen method for samples, then the value of the total protein was calculated by multiplying the nitrogen value by a factor of 6.25. Carbohydrates were measured according to the following equation:

$$Carbohydrates\,(\%) = 100 - [moisture\% + ash\% + protein\% + fat\%] \quad (23)$$

2.15 | Statistical analyses

A one-way experiment in complete randomized design (R.I.D. 60°C, R.I.D. 70°C, R.I.D. 80°C, and conventional drying) was used to analyze the influence of drying temperatures levels using R.I.D. (60, 70, and 80°C) and conventional dryer. Each treatment with three replicates was excuted. The influence of each variable on the studied characteristics (moisture content, drying rate, L^*, a^*, b^*, ΔE, ΔC, h, S.E.C., BI,

and chemical composition) was analyzed. The IBM-SPSS Statistics (version 25) analyzed experimental data, and the means of the treatments were compared by the revised least significant difference at the significance level of 0.05.

3 | RESULTS AND DISCUSSION

3.1 | Moisture content

Figure 4 depicted that the MC was decreased as drying time increased at all drying temperatures. When drying time increased from 0 to 200 min., the MC decreased from 2.33 to 0.167 g_{water}/g dm, respectively, at the drying temperature of 80°C. The highest reduction in MC was found to be at a temperature of 80°C. The required reach equilibrium moisture content (final MC) was 270, 225, and 195 min. At temperatures of 60, 70, and 80°C, respectively, as illustrated in Figure 4. It was pointed out that the increasing drying temperature from 60 to 80°C was saved 42.10% of drying time. Namsanguan, Tia, Devahastin, and Soponronnarit (2004) stated that the required time to reduce the MC of shrimp from 40 to 20% was 180 min.

The results illustrated that increasing drying temperature led to a decrease in the MC of shrimp. This is because increasing osmotic pressure of water. Murali et al. (2021) stated that the required time to decrease the MC of shrimp from 76.71 to 15.38% was 6 hr. On the other hand, the drying curve (Figure 4) showed that the conventional drying of shrimp had a higher drying time (300 min) than the R.I.D. due to the hardening surface, which late moisture exit from the product quickly. In this study, the drying time of shrimp by R.I.D. was lower than dried shrimp by solar and hot air dryer by Akonor et al. (2016), who found the required time to dry shrimp was 16 and 20 hr, respectively.

3.2 | Thermal efficiency

Figure 5 illustrated that the highest thermal efficiency was 89.53% using drying temperature of 70°C, and the lowest was 83.01% at 80°C dryi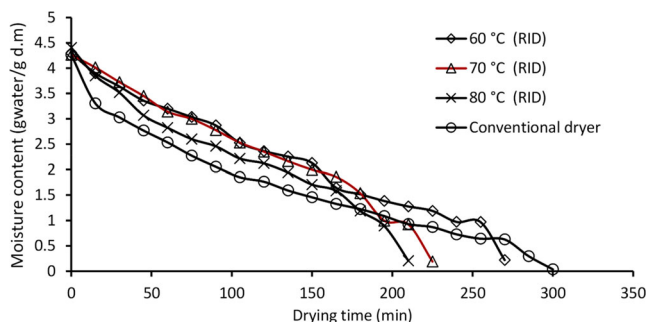ng temperature because of increase of heat loss with the increase of drying temperature. In general, the thermal efficiency was considered high, and this is because the three methods of heat transfer, namely radiation, conduction, and convection, all participated simultaneously in the drying process, in addition to the movement of air in the dryer by the fan and rotation the drying cylinder which led to the high values of efficiency. In the current study, the thermal efficiency of R.I.D. was higher compared with other dryers.

3.3 | Drying rate

Figure 6 depicted the drying rate versus moisture content at different drying temperatures. The results showed that the drying rate of dried shrimp by R.I.D. consists of only a falling rate period at all drying temperatures (60, 70, and 80°C) and no constant rate observed because of high protein content in shrimp which leads to holding water resulting reduce free water. This clarified that the transfer of moisture in shrimp occurs by the process of diffusion. These results agreed with Murali et al. (2021), who stated that only the falling rate period represented the drying process of shrimp dried by solar energy.

Moreover, moisture diffusion from the inner part of foods is toward controlling the drying rate (Al-Hilphy et al., 2021). It can be seen from Figure 6 that the drying rate consisted of three parts of the falling rate period for all drying temperatures. That is, at 80°C, the first part began from moisture content of 3.848–3.028 g_{water}/g dm, the second part was noticed for the moisture content of 3.028–2.534 g_{water}/g dm, and the third part was observed for the moisture content of 2.534–0.204 g_{water}/g dm.

Figure 7 illustrates the effect of the drying temperature of shrimp on the drying rate. The results showed that the drying rate significantly ($p < .05$) increased as drying temperature increased because of increasing evaporated water from shrimp to air drying with increasing drying temperature. Al-Hilphy et al. (2021) stated that the drying temperature significantly affects the drying rate. Murali et al. (2021) dried shrimp by a solar dryer at 54°C, and it was found that the drying rate reduced from 0.7 to 0.05 kg/kg dm. h with increasing time from 10:30 a.m. to 4:30 p.m., respectively. The relationship between drying temperature and drying rate was a polynomial model (Equation (24),
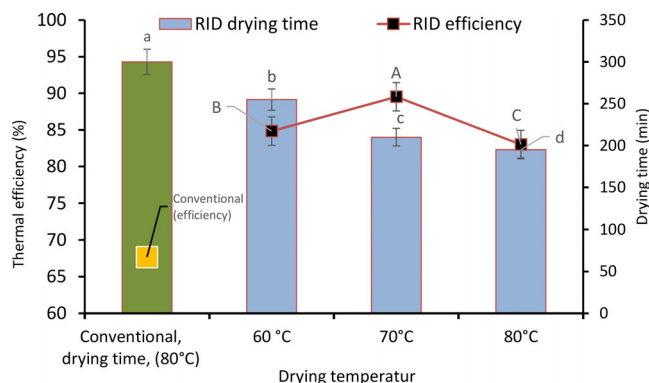
FIGURE 4 Drying curves of shrimp dried by rotary infrared dyer at temperatures of 60, 70, 80°C, and conventional

FIGURE 5 Drying time and efficiency of shrimp dried using a rotary infrared dryer at different drying temperatures
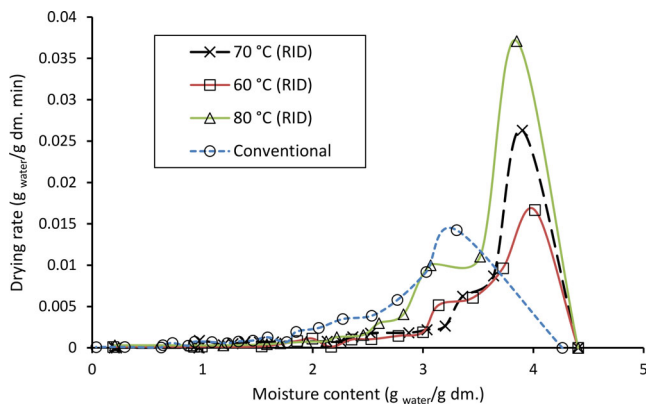
FIGURE 6 Drying rate versus moisture content at different drying temperatures
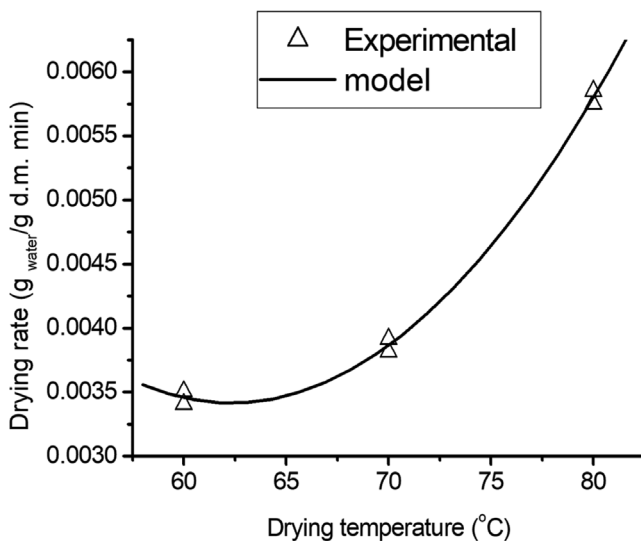

FIGURE 7 Mean drying rate versus drying temperature (dm, dry matter)

and the statistical parameters of the polynomial model extracted using Microcal Origin software (mathematical modeling program) were $R = .99834$, $SD = 7.07107E\text{-}4$, and $p = 1.16857E\text{-}4$.

$$DR = 0.03301 - 9.49692 \times 10^{-4}T + 7.62005 \times 10^{-6}T^2 \quad (24)$$

where DR is the drying temperature (g_{water}/g dm/min) and T is the drying temperature (°C). The maximum drying rate of dried shrimp using a conventional dryer was 0.0639 g_{water}/g dm, then reduced with decreasing moisture content.

3.4 | Mathematical modeling

Table 3 illustrates the mathematical thin layer models and statistical parameters of shrimp moisture ratio at drying temperatures of 60, 70,

and 80°C. The results depicted that the logarithmic model processes and proposed model (exponential) were well fitted at a drying temperature of 60°C according to the statistic parameters, which gave a higher R^2 (.996773 and .996723, respectively) and lower RMSE (0.023803 and 0.024036, respectively) compared to the other models at 60°C temperature. Moreover, Page model, Approximation of diffusion, Wang and Singh, Midilli, ANN, Verma, Modified, and Henderson can be used to fit experimental data because they have R^2 and RMSE ranging from 0.98857 to 0.99648, and 0.025677 to 0.04578, respectively. Modified Henderson and Pabis model best fitted at 70 and 80°C temperatures ($R^2 = .996411$ and .999272; RMSE = 0.024767 and 0.010548, respectively) compared to other models at these drying temperatures. The results revealed that the ANN, proposed, Verma et al., Midilli, Wang and Singh, Approximation of diffusion, Logarithmic model have a good fitting at 70 and 80°C temperature because R^2 and RMSE were ranged between .993446 and .996971 and 0.026236 and 0.03242, respectively, at 70°C temperature and ranged from 0.990927 to 0.995634 and 0.025805 to 0.045659, respectively.

In the present study, the models of Logarithmic, the proposed model (exponential), Page, Approximation of diffusion, Wang and Singh, Midilli, ANN, Verma, Modified, and Henderson were used to predict the moisture ratio at drying temperature of 60, 79, and 80°C by a fitting curve as clarified in Figure 8. The curve fitting between predicted and experimental data using Logarithmic, the proposed model (exponential), Page, Approximation of diffusion, Wang and Singh, Midilli, ANN, Verma, Modified, and Henderson at temperatures of 60, 70, and 80°C were better than the other models due to it has the highest values of R^2 and lowest values of RMSE. Figure 9 illustrated that experimental and predicted moisture ratio according to the transient moisture diffusivity equation at 60, 70, and 80°C.

3.5 | Mass transfer coefficient

Table 4 shows the lag factor, drying coefficients (S and A), statistical parameters, and mass transfer parameters (Bi, μ, D, and h) of shrimp drying. The drying coefficient has a direct impact on moisture diffusivity. The highest drying coefficient was 1.68×10^{-4} 1/s at a temperature of 80°C, and the lowest was 1.47×10^{-4} 1/s at a temperature of 60°C, which means that drying temperature has a direct effect on the drying kinetics. Costa, Silva, Silva, and Rodrigues (2018) reported that the S value ranged between 1.43 and 2.76 1/s for drying shrimp using convective tray dryer.

Dincer and Dost (1996) stated that the lag factor (A) is considered an indicator of increasing internal resistance to transfer of moisture, and it has a direct effect on the coefficient of moisture transfer. In addition, Biot number (Bi) should be considered. The results in Table 4 illustrates that the Bi value ranged between 1.0040 and 1.0826, which was the range in 0.1 < Bi < 10.0 at 60 and 70°C temperature, this means that the internal and external resistance were present, but it was lower than 0.1 at 70°C temperature (0.01359). Costa et al. (2018) depicted that Bi for drying shrimp ranged between 0.1351 and

TABLE 3 Mathematical models coefficients (constants) and statistic parameters of shrimp moisture ratio at deferent drying temperatures using the rotary infrared dryer

Model	Temperature	Constants		R^2	RMSE
Lewis model	60	k	0.00832	.98012	0.07010
	70	k	0.00803	.97220	0.07994
	80	k	0.01003	.98464	0.04932
Al-Hilphy et al.	60	k	6.43E-06	.94528	0.14150
		a	0.99999		
		c	−0.00054		
	70	k	7.43E-06	.94165	0.15006
		a	0.99999		
		c	−0.0006		
	80	k	5.94E-06	.98470	0.04934
		a	1.000		
		c	0.00059		
Page model	60	k	0.0012	.98857	0.04579
		n	1.39665		
	70	k	0.000697	.98353	0.05128
		n	1.50531		
	80	k	0.00696	.985163	0.047827
		n	1.078855		
Modified page model	60	k	0.002584	.980133	0.071994
		n	3.220748		
	70	k	0.002539	.972206	0.08214
		n	3.164876		
	80	k	0.002837	.984649	0.049325
		n	3.536879		
Henderson and Pabis	60	k	0.008828	.977205484	0.068622
		a	1.058939		
	70	k	0.008765	.972206	0.076300
		a	1.004027		
	80	k	0.010081	.984528	0.049300
		a	1.004027		
Logarithmic model	60	a	1.976343	.996773	0.023803
		k	0.002755		
		c	−0.99867		
	70	a	8.495861	.995704	0.026367
		k	0.00056		
		c	−7.51175		
	80	a	1.448535	.991739	0.035463
		k	0.00486		
		c	−0.49647		
Two-term model	60	a	1.056514	.978167	0.064608
		b	0.000544		
		k_o	0.008666		
		k_1	0.008666		
	70	a	1.08214	.967786	0.074265
		b	0.000544		
		k_o	0.008766		
		k_1	0.008766		

(Continues)

TABLE 3 (Continued)

Model	Temperature	Constants		R^2	RMSE
	80	a	1.003488	.984529	0.0493
		b	0.000538		
		k_o	0.010081		
		k_1	0.01007		
Approximation of diffusion	60	a	2.256728	.996627	0.025677
		b	0.188252		
		k_o	0.002891		
	70	a	5.15446	.995611	0.027686
		b	0		
		k_o	0.000978		
	80	a	1.277064	.990928	0.038977
		b	0		
		k_o	0.006571		
Wang and Singh	60	a	−0.0056	.996748	0.025881
		b	6.41E-06		
	70	a	−0.00481	.995699	0.028431
		b	1.1E-06		
	80	a	−0.00721	.990195	0.045659
		b	1.23E-05		
Midilli	60	a	1.002051	.994763	0.031138
		b	−0.00374		
		n	0.027831		
		k	0.09916		
	70	a	1.001884	.995971	0.026236
		b	−0.00414		
		n	0.422518		
		k	0.009954		
	80	a	1.003258	.995634	0.025805
		b	−0.00278		
		n	0.490661		
		k	0.040076		
Two-term exponential	60	a	1.002051	.980921	0.069695
		k	0.008179		
	70	a	1.002051	.972206	0.08214
		k	0.008035		
	80	a	1.002051	.984649	0.049325
		k	0.010035		
Verma et al.	60	a	2.453843	.996628	0.025679
		k	0.002785		
		g	0.000687		
	70	a	5.162249	.995611	0.027686
		k	0.000976		
		g	0		
	80	a	1.276908	.990927	0.038977
		k	0.006572		
		g	0		

TABLE 3   (Continued)

Model	Temperature	Constants		R^2	RMSE
Modified Henderson and Pabis	60	*a*	0.474638	.996761	0.024499
		k	0.003115		
		g	−0.00045		
		b	−0.70625		
		c	1.209839		
		h	0.003043		
	70	*a*	−1.93184	.996411	0.024767
		k	−0.00229		
		g	−0.00072		
		b	2.709267		
		c	0.231105		
		h	0.018625		
	80	*a*	−0.23619	.999272	0.010548
		k	−0.01255		
		g	−0.01021		
		b	0.364516		
		c	0.871885		
		h	0.013749		
Simplified Fick's diffusion	60	*a*	1.057059	.978166	0.066379
		c	0.004296		
		L	0.704119		
	70	*a*	1.082683	.967786	0.0763
		c	0.004306		
		L	0.700893		
	80	*a*	1.004028	.984528	0.0493
		c	0.004413		
		L	0.661633		
ANN	60	*a*	0.952	.995508	0.028143
		b_1	−0.0033		
		b_2	−2E-07		
		b_3	1E-07		
		b_4	−2E-10		
	70	*a*	0.9689	.99418	0.030794
		b_1	−0.0038		
		b_2	−0.00001		
		b_3	5E-08		
		b_4	−3E-11		
	80	*a*	0.9506	.990939	0.037954
		b_1	−0.007		
		b_2	0.00001		
		b_3	4E-08		
		b_4	−1E-10		
The proposed model (exponential)	60	*a*	1.552005	.996723	0.024036
		b	570.8102		
		c	−357.073		

(Continues)

TABLE 3 (Continued)

Model	Temperature	Constants		R^2	RMSE
	70	a	1.13876	.993446	0.03282
		b	349.379		
		c	−296.999		
	80	a	3.428432	.988994	0.041027
		b	1,691.032		
		c	−486.32		

Note: a, b, c, b_1, b_2, b_3, b_4, L, h, g, k, n, k_1, and k_o are constants, R^2, determination coefficient.
Abbreviations: AAN, artificial neural network; RMSE, root mean square error.
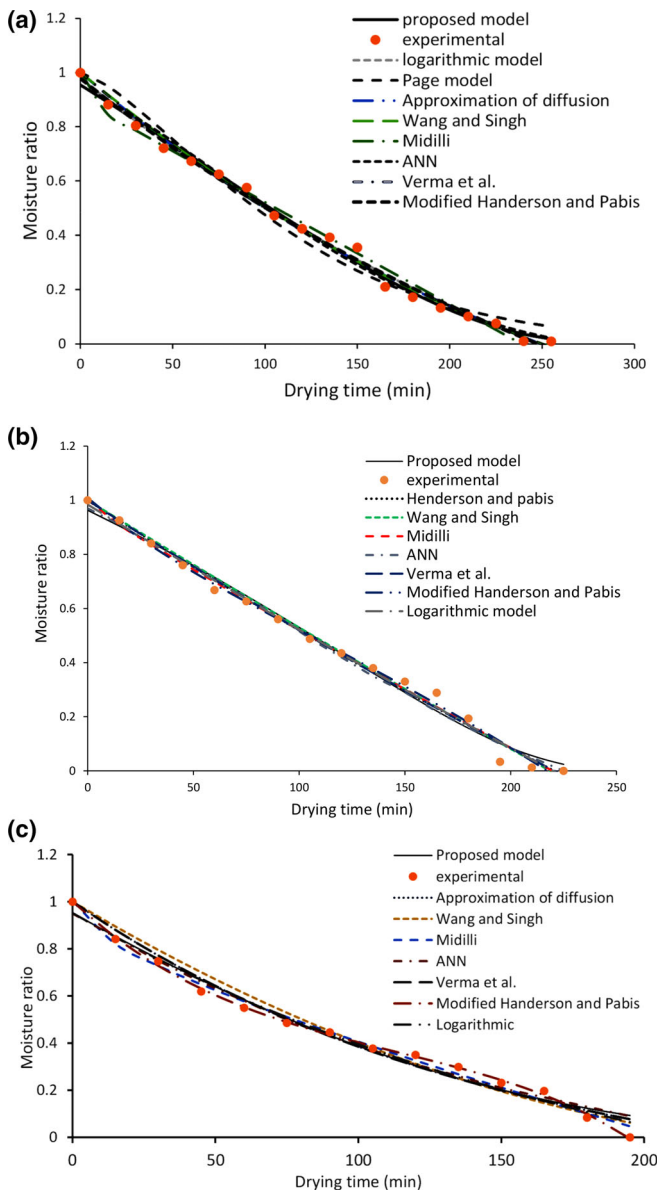

FIGURE 8 Experimental and predicted moisture ratio according to deferent models at temperatures of 60 (a), 70 (b), and 80°C (c)
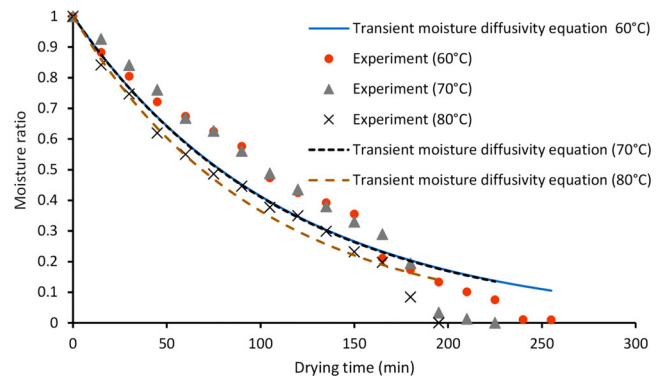

FIGURE 9 Experimental and predicted moisture ratio according to transient moisture diffusivity equation at temperatures of 60, 70, and 80°C

0.1430 due to use different pretreatments (boiling, salt solution, and smoking) for shrimp before drying. In addition, μ depends on the Bi, which is directly affected by Bi, as illustrated from results in Table 4.

For moisture diffusivity (D), the results in Table 4 showed that the D value was increased as drying temperature increased, and the highest and lowest D value was 3.245×10^{-6} and 1.023×10^{-8} at the temperature of 80 and 60°C, respectively. Costa et al. (2018) found that the D value of dried shrimp using convective tray dryer ranged between 1.01×10^{-8} and 2.05×10^{-8} m²/s. In this study, the D value at 80°C was higher than in some literature. This variation depends on the experimental procedure's types and conditions used to determine the D, data treatment methods, structure complexity of foods, drying temperature, physical or chemical pretreatment, and moisture content (Shi, Zheng, & Zhao, 2013). As for moisture transfer coefficient (h), the results clarified that the h was increased with the increase of drying temperature, that is, h increased from 1.108×10^{-6} to 2.210×10^{-6} m/s when drying temperature increased from 60 to 80°C, respectively. The value of h is critical in assessing simultaneous heat and mass transfer processes (Costa et al., 2018).

TABLE 4 Lag factor, drying coefficient (A and S), statistical parameters, and mass transfer parameters (Bi, μ, D, and h) of shrimp drying

Drying method	S (1/s)	A	R^2	X^2	Bi	μ	D	h
60 R.I.D.	1.47E-04	1.0589	.9772	0.00470	0.21666	0.7583	1.023E-07	1.108E-06
70 R.I.D.	1.48E-04	1.0526	.9677	0.00582	0.19171	0.7153	1.157E-07	1.109E-06
80 R.I.D.	1.68E-04	1.0040	.9845	0.00243	0.01359	0.1439	3.245E-06	2.210E-06

Note: S: drying coefficient, A: lag factor, R^2: determination coefficient, χ^2: chi-square, Bi: Biot number, μ: dimensionless, D: moisture diffusion and h: moisture transfer coefficient.
Abbreviation: R.I.D., rotary infrared dryer.
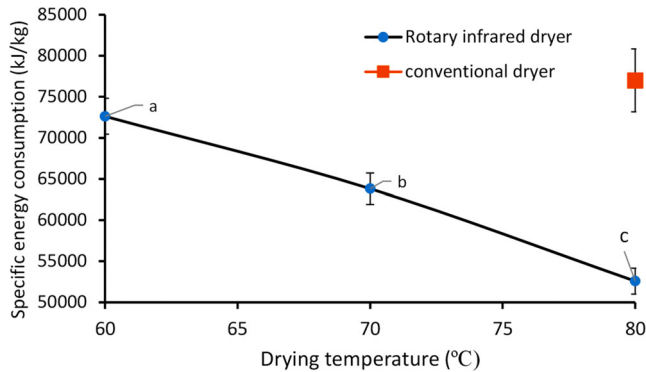
FIGURE 10 Specific energy consumption (S.E.C.) of drying shrimp using the rotary infrared dryer and conventional dryer versus drying temperature

3.6 | Specific energy consumption

Figure 10 shows S.E.C. of drying shrimp using the R.I.D. The results showed that the S.E.C. was decreased as drying temperature increased. This is due to a decrease in the required time for drying with increasing drying temperature. The maximum and minimum S.E.C. were 72,626.58 and 52,587.15 kJ/kg at drying temperatures of 60 and 80°C, respectively. Khan, Moradipour, Obeidullah, and Quader (2020) depicted that S.E.C. freshwater fishes processed by forced convective air dryer were increased with increasing drying time. S.E.C. of drying shrimp using conventional dryer was higher than the R.I.D. by 46.42%. This is because of the increase in the energy requirements and increased drying time.

3.7 | Color characteristics of dried shrimp

Table 5 illustrates the effect of drying temperature on color characteristics of dried shrimp by the R.I.D. The results showed that the drying temperature had a significant effect ($p < .05$) on the qualities of the color of L^*, a^*, b^*, ΔE, ΔC, and h of shrimp, and they were greater at a temperature of 70°C compared with the temperature of 60 and 80°C as it reached 77.74, where the color became lighter than the fresh shrimp, but at 80°C, gave a slightly darker color than the fresh shrimp, due to the high temperature of the shrimp. The color of the dried shrimp at 60°C was darker due to the long drying time and a long time of exposure to infrared radiation.

The results also showed that b^* was significantly ($p < .05$) affected by temperature, as it increased to 50.82 at 60°C temperature compared to fresh shrimp, while it decreased significantly ($p < .05$) at 70 and 80°C, and the reason for this difference may be because of temperature that increased L^* and inclined a^* and b^*.

Niamnuy, Devahastin, Soponronnarit, and Raghavan (2008) stated that the astaxanthin, a carotenoid, in dried shrimp increased with temperature. The researchers found that Astaxanthin was higher at temperatures of 100 and 120°C compared with 80°C because the required time for drying is lower at a higher temperature. Astaxanthin is sensitive to oxidation due to its highly unsaturated structures. In shrimp oil, oxygen availability, light, air, and temperature affect astaxanthin degradation and lipid oxidation (Takeungwongtrakul & Benjakul, 2016). The isomerization of natural astaxanthin to [Z]-isomeric forms, especially to 9-[Z] and 13-[Z] isomers. [Z]-isomers are characterized by lower bioavailability and stability, especially in the presence of light, oxygen, or high temperature (Stachowiak & Szulc, 2021). Therefore, such a phenomenon might be involved during shrimp drying and color changes that were observed in the present study.

The total change of color (ΔE) was highest at 70°C, then 60°C, followed by 80°C. Chroma (ΔC) was higher at a temperature of 60°C. The ΔE and ΔC increased significantly ($p < .05$) with the increase in the drying temperature from 70 to 80°C due to the nonenzymatic reactions resulting from the temperature increase. The hue angle (h) was decreased significantly ($p < .05$) with the increase in the drying temperature, because of exposure to infrared radiation, which raised the surface temperature of the food (increased a^* value) and led to its color change. At a temperature of 70°C, the h increased significantly ($p < .05$). The dried shrimp by conventional dryer gave a lower L^*, a^*, and b^* values, and higher values of ΔE, ΔC, and h compared to the R.I.D. because the heat transfer from the surface toward the inner of shrimp, which led to overheating on the surface of shrimp.
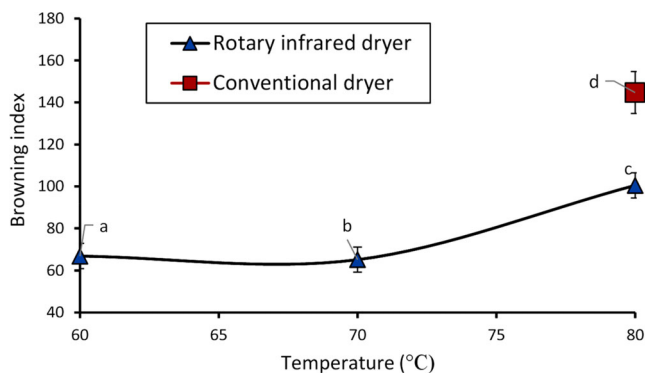
3.8 | Browning index

Figure 11 shows the effect of the drying temperature on the BI of the dried shrimp by the R.I.D. The results showed that the BI significantly ($p < .05$) increased with the increase of the drying temperature. When the drying temperature was 60, 70, and 80°C, the BI reached 66.82, 65.13, and 100.48, respectively. This is due to the intensity of the infrared ray, which led to an increased BI as a result of the

TABLE 5 Color characteristics of dried shrimp by the rotary infrared dryer and conventional

Dying temperature	L*	a*	b*	ΔE	ΔC	h
Fresh	66.86 ± 2.10[b]	16.94 ± 0.98[c]	36.71 ± 1.23[b]	—	—	65.26 ± 2.78 [a]
R.I.D. 60	59.411 ± 1.56[d]	19.76 ± 0.87[d]	50.82 ± 2.23[a]	16.20 ± 2.12[a]	14.39 ± 1.23[a]	68.78 ± 3.01[c]
R.I.D. 70	77.84 ± 2.44[a]	24.00 ± 1.02[b]	27.29 ± 2.33[d]	29.33 ± 1.78[b]	11.76 ± 0.78[c]	48.72 ± 2.87 [b]
R.I.D. 80	63.73 ± 1.98[c]	30.12 ± 1.11[a]	31.53 ± 1.98[c]	14.21 ± 0.98[c]	14.16 ± 097[b]	46.43 ± 1.98[b]
Conventional dryer	41.37 ± 2.05[e]	15.52 ± 0.99[e]	30.11 ± 1.01[c]	29.63 ± 0.99[b]	15.12 ± 1.03[d]	62.75 ± 2.06[a]

Note: The different letters in the same column refer to significant differences at .05 level.
Abbreviations: *h*, hue angle; R.I.D., rotary infrared dryer.

FIGURE 11 Browning index of dried shrimp by a rotary infrared dryer (R.I.D.) and conventional dryer versus drying time

FIGURE 12 Rehydration of dried shrimp using the rotary infrared dryer (R.I.D.) and conventional versus time
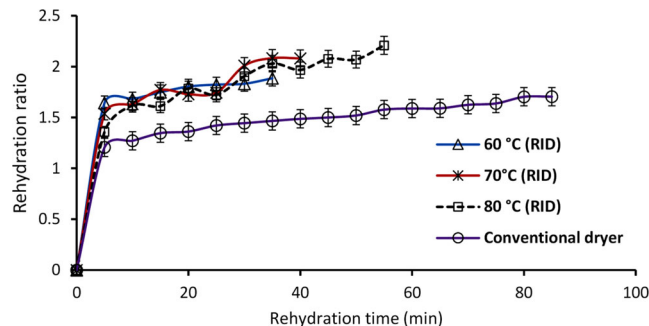
concentration of rays on the surface of the food, which led to a rise in food surface temperature more than inside food led to the formation nonenzymatic that increased BI. In order to understand the effect of temperature more accurately, Equation (25) shows the possibility of predicting a BI (BI_{sh}) at any drying temperature (*T*).

$$BI_{sh} = 0.1853T^2 - 24.256T + 855.18; R^2 = .999 \qquad (25)$$

The results showed that the BI of dried shrimp using a conventional dryer was higher by 43.99% than the R.I.D. This is because of the longtime of drying shrimp by the conventional dryer.

3.9 | Rehydration

Figure 12 depicts the rehydration of dried shrimp by the R.I.D. The rehydration increased with the increase of rehydration time, and the dried shrimp required more time at temperatures 80°C compared to 60 and 70°C. For example, at temperatures 60, 70, and 80°C, the rehydration time for dried shrimp was 35, 40, and 55 min, respectively. This is due to the surface hardening of the dried shrimp at 80°C, which impeded the absorption of water. The rehydration was 1.88, 2.08, and 2.20 when using temperatures 60, 70, and 80°C, respectively. This relative increase in the rehydration was due to the prolonged stay of the dried product in water. Namsanguan et al. (2004) reported that the rehydration of dried shrimp by the superheated

steam dryer and heat pump dryer increased, and rehydration increased as rehydration time increased. The rehydration ratio of shrimp dried by a conventional dryer was lower than that of the R.I.D. The rehydration of dried shrimp in this study was higher than the earlier studies, that is, Akonor et al. (2016) reported that the rehydration ratio of dried shrimp reached 1.90, 1.88 for air oven and solar dryers, respectively.

3.10 | Chemical composition

Regarding the chemical composition, Table 6 shows the chemical characteristics of the R.I.D. and the conventional dried samples, where the results showed significant differences (*p* < .05) between R.I.D. and the conventional. That is, the moisture content and protein of shrimp dried by R.I.D. were higher compared with the conventional dryer, which reached 18 and 15% moisture content, and 56.65 and 51.56%, respectively. On the other hand, ash, fat, and carbohydrate were lower than the conventional dryer and reached 1.29, 1.31, and 17.88%, respectively, using R.I.D., and reached 6.8, 1.6, and 22.1%, respectively, using the conventional dryer. This is because the moisture content and protein of dried shrimp by R.I.D. were higher than the conventional. The moisture content and protein of dried shrimp were lower than the R.I.D in the conventional drying. On the other hand, ash, fat, and carbohydrate content increased. This could be related to differences in the final moisture content values of samples as well as possibility of different patterns of thermal degradation

TABLE 6 chemical composition of raw and dried shrimp by infrared and conventional dryers at 80°C

Properties (%)	Raw shrimp	Dried shrimp	
		Dried by R.I.D.	Dried by conventional dryer
Moisture content	81.10 ± 3.34[a]	18 ± 1.04[b]	15.00 ± 1.03[c]
Protein	17.00 ± 1.54[c]	56.65 ± 2.54[a]	51.56 ± 1.37[b]
Ash	1.29 ± 0.02[c]	6.11 ± 0.89[b]	6.80 ± 0.86[a]
Fat	0.31 ± 0.012[c]	1.10 ± 0.03[b]	1.60 ± 0.78[a]
Carbohydrate	0.084 ± 0.01[c]	17.88 ± 0.95[b]	22 ± 1.01[a]

Note: The different letters in the same column refer to significant differences at .05 level.
Abbreviation: R.I.D., rotary infrared dryer.

during different thermal drying conditions. Costa et al. (2018) found that the moisture, fat, protein, and ash content of fresh shrimp 73.4, 2.3, 22.7, and 1.6, respectively, and dried shrimp by convection tray dryer 15.92, 10.34, 0.96, and 51.07%, respectively. These results compare well with 86.21%, 10, and 10% moisture content of fresh shrimp, air ovendried, and solar dried, respectively, reported in the previous study (Akonor et al., 2016). In addition, Ajifolokun, Basson, Osunsanmi, and Zharare (2018) reported that the moisture, ash, protein, fat, and carbohydrate of dried shrimp by sun-drying reached 13.7, 6.77, 58.4, 1.98, and 18.41%, respectively.

3.11 | The operating cost of the R.I.D. for shrimp drying

The power of R.I.D. and conventional dryer in this study were estimated to be 0.25 and 0.8 kW, respectively. The saved power by R.I.D. is then about 0.55 kW. It can be assumed that the annual saving cost ($/year) = total power saving (kW) × annual hours (hr/year) × cost (0.067 $/kWh) = 114.41 $/year. According to the above-mentioned assumption, the annual cost of R.I.D. and the conventional dryer are expected to be 52 and 166.43 $/year, respectively. This means that the R.I.D. can probably reduce the cost by about 61.9%.

4 | CONCLUSIONS

The thermal efficiency of the infrared dryer was decreased as drying temperature increased, and it was higher than the conventional dryer. The drying rate of dried shrimp by R.I.D. consists of only a falling rate at all drying temperatures. The models of logarithmic, the proposed model (exponential), Page, Approximation of diffusion, Wang and Singh, Midilli, ANN, Verma, Modified, and Henderson were used to predict the moisture ratio at drying temperature of 60, 70, and 80°C. Mass transfer coefficient was increased with the increase of drying temperature. S.E.C. was decreased as drying temperature increased. The color components were changed with changing temperature and drying method. The BI of dried shrimp using a R.I.D. was lower compared to the conventional dryer. The rehydration of dried shrimp by

R.I.D. required added time at 80°C compared to 60 and 70°C with a higher rehydration ratio than the conventional dryer.

CONFLICT OF INTEREST
The authors declare no potential conflict of interest.

AUTHOR CONTRIBUTIONS
Asaad R. Al-Hilphy: Conceptualization; data curation; formal analysis; funding acquisition; investigation; resources; software; supervision; visualization. **Atheer Abdul Amir Al-Mtury**: Formal analysis; methodology. **Sajeda A. Al-Iessa**: Investigation. **Sabah Malik Al-Shatty**: Data curation; investigation. **Mohammed Ali Jassim**: Resources; visualization. **Zainab Abdul Ameer Mohusen**: Investigation; project administration; software. **Amin Mousavi Khaneghah**: Supervision; revision; editing.

DATA AVAILABILITY STATEMENT
Data are not shared.

ORCID
Asaad R. Al-Hilphy https://orcid.org/0000-0001-5850-1519
Mohsen Gavahian https://orcid.org/0000-0002-4904-0519
Amin Mousavi Khaneghah https://orcid.org/0000-0001-5769-0004

REFERENCES
Aboud, S. A., Altemimi, A. B., Al-Hilphy, R. S. A., Yi-Chen, L., & Cacciola, F. (2019). A comprehensive review on infrared heating applications in food processing. *Molecules*, *24*(22), 4125. https://doi.org/10.3390/molecules24224125

Ajifolokun, O. M., Basson, A. K., Osunsanmi, F. O., & Zharare, G. E. (2018). Effects of drying methods on quality attributes of shrimps. *Journal of Food Processing and Technology*, *10*, 772. https://doi.org/10.4172/2157-7110.1000772

Akonor, P. T., Ofori, H., Dziedzoave, N. T., & Kortei, N. K. (2016). Drying characteristics and physical and nutritional properties of shrimp meat as affected by different traditional drying techniques. *International*

Journal of Food Science, 2016, 1–5. https://doi.org/10.1155/2016/7879097

Al-Hilphy, A. R., Gavahian, M., Barba, F. J., Lorenzo, J. M., Al-Shalah, Z. M., & Verma, D. K. (2021). Drying of sliced tomato (Lycopersicon esculentum L.) by a novel halogen dryer: Effects of drying temperature on physical properties, drying kinetics, and energy consumption. *Journal of Food Process Engineering, 44*(3), e13624. https://doi.org/10.1111/jfpe.13624

Aniesrani Delfiya, D. S., Murali, S., Alfiya, P. V., & Samuel, M. P. (2020). Drying characteristics of shrimp (Metapenaeus dobsoni) in electrical dryer. *Pantnagar Journal of Research, 18*(3), 280–284. http://krishi.icar.gov.in/jspui/handle/123456789/46039

AOAC International. (2016). *Official methods of analysis of AOAC International* (20th ed., p. 3172). Rockville, MD: AOAC International. http://www.eoma.aoac.org/methods/info.asp?ID=16264. ISBN: 978-0-935584-87-5.

Costa, M. V. D., Silva, A. K. N. D., Silva, L. H. M. D., & Rodrigues, A. M. D. C. (2018). Prediction of moisture transfer parameters for convective drying of shrimp at different pretreatments. *Food Science and Technology, 38*, 612–618. https://doi.org/10.1590/fst.31517

Delfiya, D. A., Prashob, K., Murali, S., Alfiya, P. V., Samuel, M. P., & Pandiselvam, R. (2021). Drying kinetics of food materials in infrared radiation drying: A review. *Journal of Food Process Engineering*, e13810. https://doi.org/10.1111/jfpe.13810

Demir, V. E. D. A. T., Gunhan, T. U. N. C. A. Y., & Yagcioglu, A. K. (2007). Mathematical modelling of convection drying of green table olives. *Biosystems Engineering, 98*(1), 47–53. https://doi.org/10.1016/j.biosystemseng.2007.06.011

Diamante, L. M., & Munro, P. A. (1993). Mathematical modelling of the thin layer solar drying of sweet potato slices. *Solar Energy, 51*, 271–276. https://doi.org/10.1016/0038-092X(93)90122-5

Dincer, I., & Dost, S. A. (1996). Modeling study for moisture diffusivities and moisture transfer coefficients in drying of solid objects. *International Journal of Energy Research, 20*(6), 531–539. https://doi.org/10.1002/(SICI)1099-114X(199606)20:6<531::AIDER171>3.0.CO;2-6

Dincer, I., & Hussain, M. M. (2002). Development of a new Bi–Di correlation for solids drying. International. *International Journal of Heat and Mass Transfer, 45*(15), 3065–3069. http://dx.doi.org/10.1016/S0017-9310(02)00031-5.

Donsì, G., Ferrari, G., & Matteo, D. I. (2021). Utilization of combined processes in freeze-drying of shrimps. *Food and bioproducts processing, 79*(3), 152–159. https://doi.org/10.1205/096030801750425244

Doymaz, I. (2011). Drying of thyme (Thymus vulgaris L.) and selection of a suitable thin-layer drying model. *Journal of Food Processing and Preservation, 35*(4), 458–465. https://doi.org/10.1111/jfpe.13564

Doymaz, İ., & İsmail, O. (2011). Drying characteristics of sweet cherry. *Food and Bioproducts Processing, 89*(1), 31–38. https://doi.org/10.1016/j.fbp.2010.03.006

Earle, R. L. (1983). *Unit operations in food processing* (2nd ed.). Oxford, England: Pergamon Press. https://nzifst.org.nz/resources/unitoperations/index.htm

Ersan, A. C., & Tugrul, N. (2020). The drying kinetics and characteristics of shrimp dried by conventional methods. *Chemical Industry and Chemical Engineering Quarterly*, 50. https://doi.org/10.2298/CICEQ201114050E

Gavahian, M., Chu, Y. H, & Farahnaky, A. (2019). Effects of ohmic and microwave cooking on textural softening and physical properties of rice. *Journal of Food Engineering, 243*, 114–140. https://doi.org/10.1016/j.jfoodeng.2018.09.010

Gökoğlu, N. (2021). Introduction to shell fish. In *Shellfish processing and preservation* (1st ed, pp. 1–6). Cham: Springer. https://doi.org/10.1007/978-3-030-60303-8

Guochen, Z., Arason, S., & Arnason, S. V. (2010). Dehydration property of shrimp (Pandalus borealis) undergoing heat-pump drying process. *International Journal of Agricultural and Biological Engineering, 2*(4), 92–97.

http://www.abepublishing.org/journals/index.php/ijabe/article/viewFile/73/92

Hendorson, S. M., & Pabis, S. (1961). Grain drying theory (I) temperature effect on drying coefficient. *Journal of Agricultural Engineering Research, 6*(3), 169–174. https://ci.nii.ac.jp/naid/10013000959/

Hernandez-Perez, J. A., Garcıa-Alvarado, M. A., Trystram, G., & Heyd, B. (2004). Neural networks for the heat and mass transfer prediction during drying of cassava and mango. *Innovative Food Science & Emerging Technologies, 5*(1), 57–64. https://doi.org/10.1016/j.ifset.2003.10.004

Hosseinpour, S., Rafiee, S., Mohtasebi, S. S., & Aghbashlo, M. (2013). Application of computer vision technique for on-line monitoring of shrimp color changes during drying. *Journal of Food Engineering, 115*(1), 99–114. https://doi.org/10.1016/j.jfoodeng.2012.10.003

Karathanos, V. T. (1999). Determination of water content of dried fruits by drying kinetics. *Journal of Food Engineering, 39*, 337–344. https://doi.org/10.1016/S0260-8774(98)00132-0

Khan, M. A., Moradipour, M., Obeidullah, M., & Quader, A. K. M. A. (2020). Heat and mass transport analysis of the drying of freshwater fishes by a forced convective air-dryer. *Journal of Food Process Engineering, 44*(3), e13574. https://doi.org/10.1111/jfpe.13574

Lewicki, P. P. (1998). Some remarks on rehydration of dried foods. *Journal of Food Engineering, 36*(1), 81–87. https://doi.org/10.1016/S0260-8774(98)00022-3

Li, H., & Chen, S. (2019). A neural-network-based model predictive control scheme for grain dryers. *Drying Technology, 38*(8), 1079–1091. https://doi.org/10.1080/07373937.2019.1611598

Madamba, P. S., Driscoll, R. H., & Buckle, K. A. (1996). The thin-layer drying characteristics of garlic slices. *Journal of Food Engineering, 29*(1), 75–97. https://doi.org/10.1016/0260-8774(95)00062-3

Menges, H. O., & Ertekin, C. (2006). Modelling of air drying of Hacıhaliloglu-type apricots. *Journal of the Science of Food and Agriculture, 86*(2), 279–291. https://doi.org/10.1002/jsfa.2340

Midilli, A. D. N. A. N., Kucuk, H. A. Y. D. A. R., & Yapar, Z. İ. Y. A. (2002). A new model for single-layer drying. *Drying Technology, 20*(7), 1503–1513. https://doi.org/10.1081/DRT-120005864

Mikulec, A., Kowalski, S., Makarewicz, M., Skoczylas, Ł., & Tabaszewska, M.(2020). Cistus extract as a valuable component for enriching wheat bread. *Lwt, 118*(108713), https://doi.org/10.1016/j.lwt.2019.108713

Momenzadeh, L., Zomorodian, A., & Mowla, D. (2011). Applying artificial neural network for drying time prediction of green pea in a microwave assisted fluidized bed dryer. *Iranian Food Science and Technology, 14*(3), 513–522. https://doi.org/10.22067/ifstrj.v6i4.9285

Murali, S., Delfiya, D. A., Kumar, K. S., Kumar, L. R., Nilavan, S. E., Amulya, P. R., ... Samuel, M. P. (2021). Mathematical modeling of drying kinetics and quality characteristics of shrimps dried under a solar–L.P.G. hybrid dryer. *Journal of Aquatic Food Product Technology, 30*(5), 561–578. https://doi.org/10.1080/10498850.2021.1901814

Namsanguan, Y., Tia, W., Devahastin, S., & Soponronnarit, S. (2004). Drying kinetics and quality of shrimp undergoing different two-stage drying processes. *Drying Technology, 22*(4), 759–778. https://doi.org/10.1081/DRT-120034261

Niamnuy, C., Devahastin, S., Soponronnarit, S., & Raghavan, G. V. (2008). Kinetics of astaxanthin degradation and color changes of dried shrimp during storage. *Journal of Food Engineering, 87*(4), 591–600. https://doi.org/10.1016/j.jfoodeng.2008.01.013

Page, G. E. (1949). Factors influencing the maximum rates of air drying shelled corn in thin layers. (Master's thesis). Purdue University, Lafayette, LA. https://www.proquest.com/openview/7aeaccbd87e789102967d22a2ad0ca56/1?pq-origsite=gscholar&cbl=18750&diss=y

Raso, J., Frey, W., Ferrari, G., Pataro, G., Knorr, D., Teissie, J., & Miklavčič, D. (2016). Recommendations guidelines on the key information to be reported in studies of application of P.E.F. technology in food and biotechnological processes. *Innovative Food Science &*

Emerging Technologies, *37*, 312–321. https://doi.org/10.1016/j.ifset.2016.08.003

Shamsuddeen, M. M., Cha, D. A., Kim, S. C., & Kim, J. H. (2020). Effects of decompression condition and temperature on drying rate in a hybrid heat pump decompression type dryer used for seafood drying. *Drying Technology*, *39*, 1–15. https://doi.org/10.1080/07373937.2020.1756842

Sharaf-Eldeen, Y. I., Blaisdell, J. L., & Hamdy, M. Y. (1980). A model for ear corn drying. *Transactions of the ASAE*, *23*(5). https://doi.org/10.13031/2013.34757

Shi, Q., Zheng, Y., & Zhao, Y. (2013). Mathematical modeling on thinlayer heat pump drying of yacon (*Smallanthus sonchifolius*) slices. *Energy Conversion and Management*, *71*, 208–216. https://doi.org/10.1016/j.enconman.2013.03.032

Silva, P. B., Nogueira, G. D., Duarte, C. R., & Barrozo, M. A. (2021). A new rotary dryer assisted by infrared radiation for drying of acerola residues. *Waste and Biomass Valorization*, *12*(6), 3395–3406. https://doi.org/10.1007/s12649-020-01222-y

Simal, S., Deya, E., Frau, M., & Rossello, C. (1997). Simple modeling of air drying curves of fresh and osmotically pre-dehydrated apple cubes. *Journal of Food Engineering*, *33*(1–2), 139–150. https://doi.org/10.1016/S0260-8774(97)00049-6

Stachowiak, B., & Szulc, P. (2021). Astaxanthin for the food industry. *Molecules*, *26*(9), 2666. https://doi.org/10.3390/molecules26092666

Takeungwongtrakul, S., & Benjakul, S. (2016). Astaxanthin degradation and lipid oxidation of Pacific white shrimp oil: Kinetics study and stability as affected by storage conditions. *International Aquatic Research*, *8*(1), 15–27. https://doi.org/10.1007/s40071-015-0120-z

Verma, L. R., Bucklin, R. A., Endan, J. B., & Wratten, F. T. (1985). Effects of drying air parameters on rice drying models. *Transactions of the ASAE*, *28*(1), 296–301. https://doi.org/10.13031/2013.32245

Wang, C. & Singh, R. A. (1978). A single layer drying equation for rough rice. ASAE Paper No. 78-3001. America Society Agricultural Engineering. St. Joseph, MI. https://scholar.google.com/scholar?hl=ar&as_sdt=0%2C5&q=A+single+layer+drying+equation+for+rough+rice&btnG=

Wrolstad, R. E., & Smith, D. E. (2017). Color analysis. In: S. S. Nielsen, (ed.), *Food Analysis*. Cham, Switzerland: Springer International. https://doi.org/10.1007/978-3-319-45776-5_31

Yağcıoğlu, A., Değirmencioğlu, A., & Çağatay, F. (1999). Drying characteristics of laurel leaves under different drying conditions. In 7th Int Congress on Agricultural Mechanization and Energy (pp. 565-569), 26–27 May, Adana, Turkey.

Yaldýz, O., & Ertekýn, C. (2001). A model for ear corn drying. *Drying Technology*, *19*(3-4). https://doi.org/10.1081/DRT-100103936

Yam, K. L., & Papadakis, S. E. (2004). A simple digital imaging method for measuring and analyzing the color of food surfaces. *Journal of Food Engineering*, *61*(1), 137–142. https://doi.org/10.1016/S0260-8774(03)00195-X